metals

MDPI

Article

An Experimental Study on the Kinetics of Leaching Ion-Adsorbed REE Deposits with Different Concentrations of Magnesium Sulfate

Min Han [1], Dan Wang [2,*], Yunzhang Rao [1,*], Wei Xu [1,3] and Wen Nie [1]

[1] School of Resources and Environmental Engineering, Jiangxi University of Science and Technology, Ganzhou 341000, China; han@jxust.edu.cn (M.H.); 7120220067@mail.jxust.edu.cn (W.X.); wen.nie@vip.tom.com (W.N.)
[2] School of Resources and Architectural Engineering, Gannan University of Science and Technology, Ganzhou 341000, China
[3] The Seventh Geological Brigade of Jiangxi Bureau of Geology, Ganzhou 341000, China
* Correspondence: 9320230072@gnust.edu.cn (D.W.); raoyunzhang@jxust.edu.cn (Y.R.)

Abstract: As an important substitute for ammonium-free leaching, magnesium sulfate is applied as a leaching agent for the mining of ion-adsorbed REE (rare earth element) deposits. Upon deriving the equation regulating the leaching kinetics on the basis of the REE "shrinking core model" during the leaching process of magnesium sulfate, we conducted leaching experiments of natural particle-sized REE deposits by applying magnesium sulfate with concentrations of 1%, 2%, 3% and 4%. Hence, the leaching efficiencies and mass transfer rates were obtained. The results show that the hybrid control equation $\frac{\mu\delta}{D_1}\alpha + \frac{3\mu r}{2D_2}\left[1 - \frac{2}{3}\alpha - (1-\alpha)^{\frac{2}{3}}\right] = \frac{3C_0M}{\rho r}$ is applicable for describing the leaching process when the concentration of magnesium sulfate is 1%; when the concentrations reach 2%, 3% and 4%, the external diffusion control equation $\alpha = kt$ is appropriate to describe the leaching processes. The leaching efficiency of REE deposits reaches over 90%, specifically, 94.65%, 97.24% and 97.98%, when the concentration of magnesium sulfate is 2%, 3% and 4%, respectively. The maximum mass transfer rate appears when the concentration of magnesium sulfate is 4%, and the leaching time is reduced by 1.96 times compared to 1% concentration of magnesium sulfate. The results provide a favorable theoretical basis for the green and efficient extraction of ion-adsorbed REEs.

Keywords: ion-adsorbed REE deposits; magnesium sulfate; kinetics; leaching efficiency; mass transfer rate

Citation: Han, M.; Wang, D.; Rao, Y.; Xu, W.; Nie, W. An Experimental Study on the Kinetics of Leaching Ion-Adsorbed REE Deposits with Different Concentrations of Magnesium Sulfate. *Metals* **2023**, *13*, 1906. https://doi.org/10.3390/met13111906

Academic Editors: Jean François Blais and Denise Crocce Romano Espinosa

Received: 6 October 2023
Revised: 10 November 2023
Accepted: 15 November 2023
Published: 18 November 2023

1. Introduction

Ion-adsorbed REE deposits, a rare earth resource unique in China [1], as its name implies, is adsorbed on the surface of clay minerals in an ionic state [2]. Leaching agents are applied to replace rare earth ions [3,4]. Thanks to its advantages of simple operation and involving no excavation, an in situ leaching (ISL) method, similar to heap leaching and pool leaching, where ore is extracted and piled up so leaching solutions can be circulated through it [5,6], has been adopted as the dominant technology [7]. Over the past few decades, ammonium sulfate, due to its merits of high efficiency, favorable selectivity and low cost, has become an important leaching agent for rare earth mining [8].

However, environmental problems, for instance, a high content of ammonia nitrogen in groundwater and surface water [9] and water body eutrophication [10,11], are nothing new by virtue of leakage of leach liquor, an insufficient exchange of ions and a rising dosage of ammonium sulfate for a maximum REE leaching efficiency [12,13]. With increasing public attention being paid to environmental issues, researchers have tried to discover alternative leaching agents. The most frequently mentioned substitute is magnesium sulfate [14,15].

For example, Wang Ruixiang [16] clarified the optimal conditions of magnesium sulfate leaching upon his investigations into the novel ammonia nitrogen-free leaching agent

with $MgSO_4$, $Al_2(SO_4)_3$, $Fe_2(SO_4)_3$, $Na_2(SO_4)_3$, $Na_2(SO_4)_3$-H_2SO_4 and the optimization of the column leaching process. With $MgSO_4$ as a leaching agent under optimal process parameters, the leaching efficiency of ion-adsorbed REE deposits reached 95%, and the leaching efficiency of impurity aluminum was 10% lower than that of $(NH_4)_2SO_4$, according to the experiments of Huang Xiaowei, Xiao Yanfei, Yi Qihui and Chen Kaihua [17–20]. Currently, the magnesium leaching agent has found industrial application in the extraction of rare earth deposits in the Chinese provinces of Guangxi and Fujian. However, the leaching efficiency of the magnesium leaching agent was lower than that of $(NH_4)_2SO_4$ [21,22]. To improve the leaching efficiency of rare earth when magnesium sulfate is used as the leaching agent, Huang Jin [23] studied its kinetics with the cup leaching method. Previous research showed that the column leaching method was more feasible because in situ leaching demands a continuous injection of leaching solution into the ore body.

On the basis of the leaching process parameters of ion-adsorbed REE deposits, we investigated the REE leaching efficiency and mass transfer rate with various concentrations of magnesium sulfate. The experimental results were analyzed in light of the dynamic theory of the "shrinking core model". In addition to be a technical stopping for the parameter selection of leaching ion-adsorbed REE deposits, the research results provide a theoretical basis for the numerical simulation of leaching REE deposits with magnesium sulfate.

2. Theory and Experimental Process

2.1. The Shrinking Core Model Theory

The ion leaching of rare earth elements is a heterogeneous reaction between a liquid containing leached cations and the solid rare earth mineral deposits [24]. Its essence is the exchange reaction between injected cations and rare earth ions adsorbed by clay mineral particles [25]. The leaching process is a typical L–S (liquid-solid) heterogeneous reaction [26]. If the granular mineral soil is assumed to be spherical, its leaching process can be described with the "shrinking core model" [27–30].

The cations in the leaching solution react with the RE cations adsorbed on the particles; hence, mineral ion leaching is a process controlled by surface reaction. This process is mainly affected by the chemical replacement rate of cations in the leaching solution and rare earth cations adsorbed on the surface of rare earth minerals. If a $MgSO_4$ solution is applied as the leaching agent, the chemical reaction equation of Mg^{2+} and RE^{3+} is expressed as the following [31,32]:

$$[Al_4(Si_4O_{10})(OH_8)]_m 2nRE^{3+}(s) + 3nMg^{2+}(aq) \rightleftharpoons$$
$$[Al_4(Si_4O_{10})(OH_8)]_m 3nMg^{2+}(s) + 2nRE^{3+}(aq)$$

In the formula, RE (ads) and Mg (ads) are in the adsorption state of RE^{3+} and Mg^{2+}, respectively.

This mathematical model is an effective tool to judge the decisive stage of leaching efficiency and describe the leaching mechanism [33].

Mathematical models of leaching kinetics, such as the Grain Model, Uniform Pore Model, Random Pore Model, Shrinking Particle Model and Shrinking Core Model, have been proposed since the 1970s. They were established according to the characteristics of solid particles and their leaching process mechanisms (Table 1) [34].

After entering the pores of the ore body through the liquid injection hole, the $MgSO_4$ solution chemically displaces rare earth ions on the surface of the RE deposit. Together with the reacted leaching solution, rare earth ions seep into the liquid collection tank. Having a bearing on the seepage of the leaching agent and ion migration, the leaching efficiency of rare earth ions is also closely related to the ion exchange reaction on the surface of the ore particles. Therefore, the leaching process of rare earth ions can be regarded as the coupling of seepage, exchange reaction and ion migration. It can be described as follows: Stage 1, the $MgSO_4$ solution reaches the outer surface of the granular liquid film by way of seepage. Stage 2, (I) after passing through the liquid film, Mg^{2+} reaches the outer surface

of the particles (external diffusion); (II) Mg^{2+} in the $MgSO_4$ solution makes contact with the clay particles in rare earth ore bodies through diffusion (internal diffusion); (III) It then chemically displaces rare earth cations adsorbed on the surface of the clay particles in the ore body. In this way, Mg^{2+}, which substitutes rare earth cations, is adsorbed by mineral soil particles; (IV) after the chemical substitution reaction between rare earth cations and Mg^{2+}, rare earth cations are desorbed from the surface of mineral soil particles (internal diffusion), while Mg^{2+} is adsorbed to the surface of mineral soil particles; (V) after exchange, the rare earth cations enter the leach liquor through diffusion (external diffusion). Stage 3: together with the leach liquor, rare earth ions seep out of the ore body. The repetition of the above three stages makes up the leaching process of rare earth ions. Among the three stages, stage 2 is the key aspect of the whole leaching process. It can be described with the "shrinking core model" (Figure 1).

Table 1. Comparison of leaching kinetics models.

Kinetics Model	Surface Morphology	Characteristics
Grain model	Porous	Deposition of products around the unreacted core; constant particle size during leaching.
Shrinking particle model	Non-porous	Total dissolution of products; change in particle size during leaching.
Shrinking core model	Non-porous	Deposition of products around the unreacted core; constant particle size during leaching.
Uniform pore model	Porous	Total dissolution of products; change in particle size during leaching.
Random pore model	Porous	-

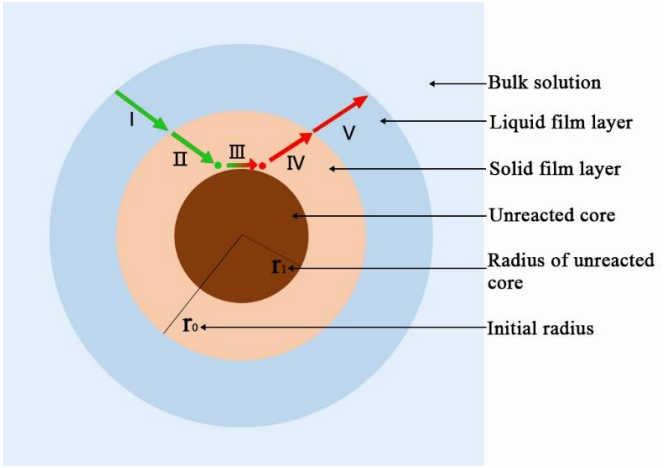

(**a**) Individual soil particle

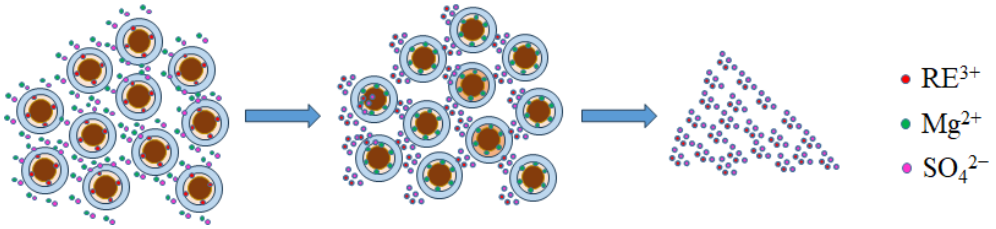

(**b**) Multiple soil particles

Figure 1. Exchange process of rare earth ions with magnesium as the leaching agent.

I. Lixiviant diffusion through liquid film layer;
II. Lixiviant diffusion through solid film layer;
III. Chemical reaction;
IV. Diffusion of products through solid film layer,
V. Diffusion of products through liquid layer [35].

In the above steps, the overall reaction rate is controlled by the chemical reaction, if the chemical reaction rate is the minimum. The following formula is applicable to the first-order reaction of rare earth ion exchange:

$$-\frac{dN}{dt} = kSC \tag{1}$$

In the formula, N is the molar amount of rare earth ions in solid particles within the specific time duration (t); S is the surface area of solid particles; C is the concentration of $MgSO_4$; K is the constant of reaction rate.

If we assume that deposit samples are dense, pore-free, spherical particles, the radius of the unreacted micronucleus is r, the density is ρ, and the molar mass is M, then the following equations can be obtained:

$$S = 4\pi r^2 \tag{2}$$

$$N = \frac{4\pi r^3 \rho}{3M} \tag{3}$$

$$-\frac{dN}{dt} = \frac{-4\pi r^2 \rho}{M} \cdot \frac{dr}{dt} \tag{4}$$

The leaching efficiency can be calculated on the basis of the following formula:

$$\alpha = \varepsilon / \varepsilon_0 \tag{5}$$

In the above formula, ε is the leached ionic-phase rare earth (g); ε_0 is the total ionic rare earth in the sample (g).

By combining the above five formulas, we can obtain the chemical reaction control equation of rare earth leaching efficiency in different time conditions.

$$1 - (1 - \alpha)^{\frac{1}{3}} = \frac{kC_0M}{\rho r_0}t \tag{6}$$

In the above formula, C_0 is the leaching agent concentration at the initial moment; r_0 is the initial radius of mineral soil particles.

If the initial concentration (C_0) of the leaching agent is constant, and $k_1 = \frac{kC_0M}{\rho r_0}$, then Formula (6) can be transformed into the following equation:

$$1 - (1 - \alpha)^{\frac{1}{3}} = k_1 t \tag{7}$$

Within a certain period of time, Mg^{2+} in the leaching solution controls the leaching speed via the diffusion rate of the liquid film on the outer surface of solid particles, if the whole leaching process is performed by external diffusion.

According to Fick's First Law, the number of moles of rare earth elements that can be extracted per unit time is calculated as follows:

$$-\frac{dN}{dt} = \frac{C_0 D_1 S}{\mu\delta} = k_2 C_0 S \tag{8}$$

In this formula, D_1 is the diffusion coefficient of $MgSO_4$ in water; S is the surface area of liquid film layer of particles.

μ is the molar ratio of Mg^{2+} passing through the liquid film layer and rare earth ions; δ is the effective thickness of the liquid film outside the mineral particles; K_2 is a constant.

When the solid film is formed or there exists inert residues, the size of mineral soil particles and liquid film on the outer wall remains almost unchanged. Then, S is a constant.

$$-\frac{dN}{dt} = \text{constant} \tag{9}$$

Though the leaching efficiency bears no relation to time, the leaching efficiency increases with the rising time duration.

Through analyzing the above formulas, we can obtain the dynamic law of external diffusion control of leaching efficiency with the variation of time:

$$\alpha = \frac{3MC_0D_1}{\mu\delta\rho r_0}t \tag{10}$$

If $k_2' = \frac{3MC_0D_1}{\mu\delta\rho r_0}$ and

$$\alpha = k_2't \tag{11}$$

In the absence of solid film and inert residue, the surface area of liquid film, which is the surface area of unreacted core, decreases with the passage of reaction time.

Then, the control dynamic equation of external diffusion is derived as follows:

$$1-(1-\alpha)^{\frac{1}{3}} = \frac{MC_0D_1}{\mu\delta\rho r_0}t \tag{12}$$

If $k_2'' = \frac{MC_0D_1}{\mu\delta\rho r_0}$ and

$$1-(1-\alpha)^{\frac{1}{3}} = k_2''t \tag{13}$$

If the leaching efficiency of rare earth ions depends on the permeability rate of Mg^{2+} passing through the solid film layer or inert residue, then the leaching reaction is subject to the internal diffusion rate.

Within a certain period of time, the molar number (J) of Mg^{2+} penetrating through the solid film layer or inert residual layer by internal diffusion is calculated as follows:

$$J = 4\pi D_2\left(\frac{r_0r_1}{r_0-r_1}\right)C_0 \tag{14}$$

In the formula, D_2 represents the diffusion coefficient of $MgSO_4$ in the solid product or inert residual layer; C_0 is the initial concentration of $MgSO_4$; r_0 stands for the initial radius of spherical mineral particles; r_1 is the core radius of unreacted soil particles.

Meanwhile, the molar number (N) of non-reactive nuclei is calculated as follows:

$$N = \frac{4\pi r_1^3\rho}{3M} \tag{15}$$

In the formula, M represents the molar mass of the solid core without participating in the reaction, and ρ is its density.

$$\frac{dN}{dt} = \frac{4\pi\rho r_1^2}{M}\cdot\frac{dr_1}{dt} \tag{16}$$

Within the unit time, the internal diffusion quantity (J) of $MgSO_4$ in the leaching solution is directly proportional to the consumption of rare earth ions.

If the proportional coefficient is supposed to be μ, then the following equation holds:

$$-\frac{MD_2C_0}{\mu\rho}dt = \left(r_1-\frac{r_1}{r_0}\right)dr_1 \tag{17}$$

After completing these calculations, we can derive the dynamic equation of the internal diffusion control between the leaching efficiency of rare earth ions and time (t):

$$1 - \frac{2}{3}\alpha - (1-\alpha)^{\frac{2}{3}} = \frac{2MC_0D_2}{\mu\rho r_0^2}t \tag{18}$$

If $k_3 = \frac{2MC_0D_2}{\mu\rho r_0^2}$, then

$$1 - \frac{2}{3}\alpha - (1-\alpha)^{\frac{2}{3}} = k_3 t \tag{19}$$

For some hybrid control systems, which have two or three speed-limiting processes in their feeding–outgoing system, the control processes are dissimilar in their initial and later stages. In spite of the substantially identical speed, different steps effect each other, thus controlling the speed of the whole reaction system. Therefore, the dynamic equation of hybrid control can be derived from the specific situations of reaction system.

In the "shrinking core model" with reduced particle size, there exists no internal diffusion stage. Such a mixed control process is jointly regulated by chemical reaction and external diffusion. By slightly treating the concentration parameters of the above formula, we can obtain the hybrid control dynamic equation of leaching efficiency (α) and time (t).

$$1 - (1-\alpha)^{\frac{1}{3}} = \frac{k_1 k}{k_1 + k}\frac{C_0 M}{r_0 \rho}t \tag{20}$$

The shrinking core model with constant particle size is divided into three control types: internal diffusion, external diffusion and chemical reaction. Effecting each other and controlling the whole reaction process, the three stages need to be determined accordingly.

The simultaneous performance of internal diffusion, external diffusion and chemical reaction appears under the following two conditions: on the one hand, their rates are basically identical at a constant concentration; on the other hand, there are certain impacts and restrictions among the three processes. The following is the dynamic equation of hybrid control:

$$\frac{\mu\delta}{D_1}\alpha + \frac{3\mu r_0}{2D_2}\left[1 - \frac{2}{3}\alpha - (1-\alpha)^{\frac{2}{3}}\right] + \frac{1}{k}\left[1 - (1-\alpha)^{\frac{1}{3}}\right] = \frac{3C_0M}{\rho r_0}t \tag{21}$$

The above formula is the sum of the three velocity formulas, and the three terms on the left represent external diffusion ($\frac{\mu\delta}{D_1}$), internal diffusion ($\frac{3\mu r_0}{2D_2}$) and surface chemical reaction ($\frac{1}{k}$), respectively. By comparing the sizes of $\frac{\mu\delta}{D_1}$, $\frac{3\mu r_0}{2D_2}$ and $\frac{1}{k}$, we can determine the control mode.

If the "shrinking core model" is adopted to describe the reaction process of ionic rare earth deposit particles, the kinetic equation of leaching is described as follows:

(1) The kinetic equation of chemical control:

$$1 - (1-\alpha)^{\frac{1}{3}} = k_1 t$$

(2) The dynamic equation of external diffusion control:

$$\alpha = k_2' t$$

(3) The dynamic equation of internal diffusion control:

$$1 - \frac{2}{3}\alpha - (1-\alpha)^{\frac{2}{3}} = k_3 t$$

(4) The dynamic equation of hybrid control:

$$\frac{\mu\delta}{D_1}\alpha + \frac{3\mu r_0}{2D_2}\left[1 - \frac{2}{3}\alpha - (1-\alpha)^{\frac{2}{3}}\right] + \frac{1}{k}\left[1 - (1-\alpha)^{\frac{1}{3}}\right] = \frac{3C_0M}{\rho r_0}t$$

2.2. Column Leaching Experiments

2.2.1. The Sampling of RE Deposits

Located in south China's Ganzhou region, the sampling point has a flat terrain, with an altitude difference of 25~35 m. The main ridge extends from north to south. With a developed weathering crust, the bedrock is exposed at the foot of the mountain. Along the Tianshui boundary of the ridge, the ore block is located on the east side of the ridge. With sparse vegetation on the surface, the topsoil has a thickness of 0~1 m. The grade of rare earth fluctuates greatly, ranging from 0.0284% to 0.1468%. With a thickness changing from 1 to 13.4 m, the ore bodies are distributed in the fully weathered granite. Their shapes and occurrences are distinctive with the variation of topography. The pattern of change is basically consistent with the topography.

For an accurate representation of the deposit sample's physical properties, we used a Luoyang shovel and spade with a diameter of 160 mm in the sampling process. Firstly, the humic layer on the surface was removed. Then, we shoveled with a spade to the depth of 0.5 m, dug 1 m at a time. With a ring knife, we took three fully weathered soil samples at the distances of 3 m, 4 m and 5 m respectively. Thus, the samples added up to 9. As too much evaporation will effect the determination accuracy of the physical properties of the sample, we packed the RE deposit samples with plastic wrap to reduce the evaporation in the subsequent transportation process. Then, we brought back the remaining loose soil at the same depth with woven bags and marked the outside of the bags. Figure 2 shows the sampling site. The samples were tested and analyzed with ICP-MS Agilent 8800. Table 2 shows the testing results. According to the test results, the grade of rare earth reaches 0.086% (g/kg), with an equivalent molar mass of 127.62 g/mol. XRD (Empyream PANalytical) analysis demonstrates that the samples are mainly composed of quartz, kaolinite, halloysite and feldspar. Figure 3 shows the major mineral components of the sample.

Figure 2. Sampling site of rare earth deposits.

Table 2. Distribution of Rare Earth Elements.

Rare earth elements	La	Ce	Pr	Nd	Sm	Eu	Gd	Tb
Contents of rare earth elements (mg/kg)	68.5	20.7	24.3	107.2	51.1	0.9	64.3	10.6
Rare earth elements	Dy	Ho	Er	Tm	Yb	Lu	Y	-
Contents of rare earth elements (mg/kg)	68.3	12.8	38.0	5.9	39.6	5.6	341.9	-

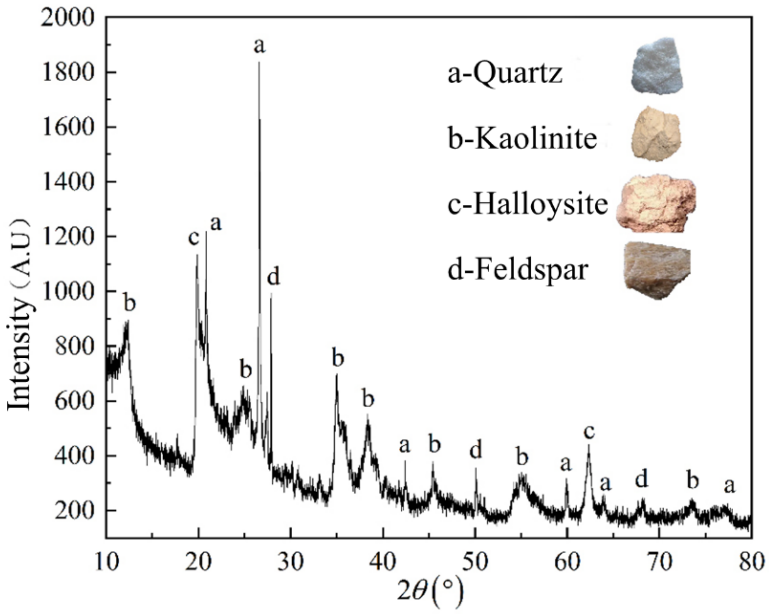

Figure 3. Major mineral components of the sample.

2.2.2. Physical Properties' Determination of the RE Deposit Samples

Table 3 shows the density of samples retrieved via the ring cutter method at different depths. As an index reflecting the development of mineral soil pores, porosity is also an important parameter of RE deposit pore structure. In the leaching process of ionic rare earth ore, the accurate measurement of porosity and void ratio is of good practical significance [36,37]. Using the parameters of gravity, density (ρ) and moisture content (ω) of the RE deposit sample, we obtained the porosity and void ratio (see Table 4). The vibrating screen method was adopted to screen the mineral soil at various depths. Sieves with different mesh numbers were stacked on a vibrating screen machine. 500 g rare earth samples at different depths were placed in the top screen. Upon vibrating the mineral deposits for 10–15 min, we weighed the quality of mineral soil on screens with different apertures. In the meantime, the percentages of each particle size range were calculated. Table 5 shows the results of the particle size distribution of the deposit samples at different depths.

Table 3. Density of deposit samples.

Depth of Deposit Samples	Serial Number	Size/cm^3	Quality/g	Natural Density/(g/cm^3)	Average Density/(g/cm^3)	Average Dry Density/(g/cm^3)
3 m	1	50.0	68.51	1.37	1.38	1.26
	2	50.0	67.85	1.36		
	3	50.0	70.38	1.41		
4 m	1	50.0	70.86	1.42	1.46	1.29
	2	50.0	74.47	1.49		
	3	50.0	73.65	1.47		
5 m	1	50.0	78.31	1.56	1.52	1.33
	2	50.0	75.62	1.51		
	3	50.0	74.23	1.48		

Table 4. Porosity percentage of void and porosity ratio of the deposit samples at different depths.

Deposit Sample Depths	3 m	4 m	5 m
Porosity percentage of void (n)	0.473	0.443	0.425
Porosity ratio (e)	0.898	0.795	0.739

Table 5. Particle size distribution of the deposit samples at different depths.

Deposit Sample Depths	Particle Diameter/mm					
	>5	2.5~5	1~2.5	0.5~1	0.075~0.5	<0.075
3 m	15.8%	32.2%	16.6%	16.2%	10.9%	8.3%
4 m	12.4%	37.3%	18.4%	16.2%	10.8%	4.9%
5 m	10.3%	31.6%	17.6%	18.2%	16.2%	6.1%
Average	12.83%	33.70%	17.53%	16.87%	12.63%	6.43%

2.2.3. Column Leaching Experiments of Natural Particle-Sized Rare Earth Deposits

(1) Pilot column leaching test

A pilot column leaching test was performed to verify the feasibility of the column leaching test. Using a Φ5 cm × 10 cm PMMA tube, we weighed 500 g deposit samples and performed column leaching experiments with clean water and then with 1%, 2%, 3% and 4% $MgSO_4$ solutions subsequently. Figure 4 shows the results. After collecting the liquid every 10 min, we tested its RE^{3+} concentration with EDTA titration [38]. The experiments were carried out at room temperature.

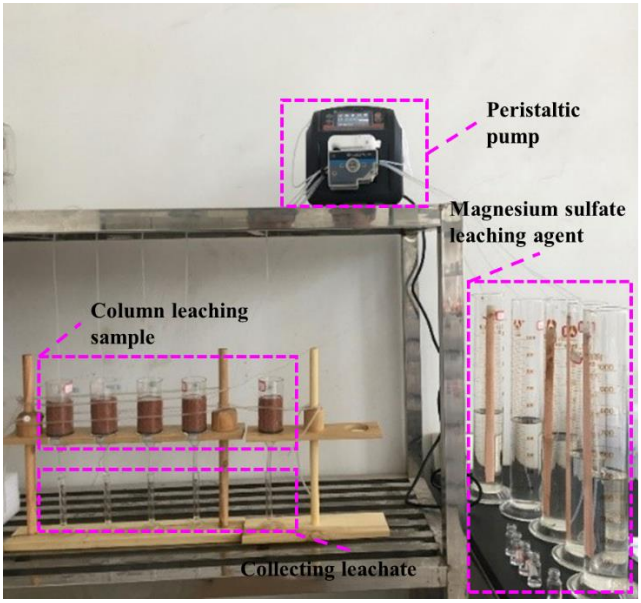

Figure 4. Pilot column leaching test.

(2) Expanded experiments of column leaching process

A self-made PMMA tube with a diameter of Φ11 cm and a length of 28 cm was used for the expansion test of the column leaching process. In accordance with the porosity ratio, we filled the RE deposit sample in the leaching column by referring to the operation regulations [39]. For uniformity of the deposit sample in the column, the tamping depth of each layer was determined to be 5 cm, with a filling depth of 20 cm. Then, the samples were vertically fixed on an iron frame. The four leaching columns were dripped with $MgSO_4$ with concentrations of 1%, 2%, 3% and 4%, respectively, as shown in Figure 5. Applying a peristaltic pump, we controlled the flow rate of the leaching solution so it was 1 mL/min. Mounted 5 cm upward from the top of the column, an overflow hole served to store the leaching agent. The pressure head was maintained at a certain level so that the leaching liquid could flow downwards at a constant speed, and the leaching column was always in a saturated state. During the experiment, the leach liquor collection and liquid injection were performed simultaneously. At the same time, the collected leach liquor was evenly mixed. A separate sampling and leach liquor collection sampling were carried out every 1.5 h. Then, their RE^{3+} concentrations were determined by EDTA titration. When

the concentration of rare earth ions in the leaching solution sampled separately was less than 0.05 g/L, we ceased injecting the liquid. This experiment was also carried out at room temperature.

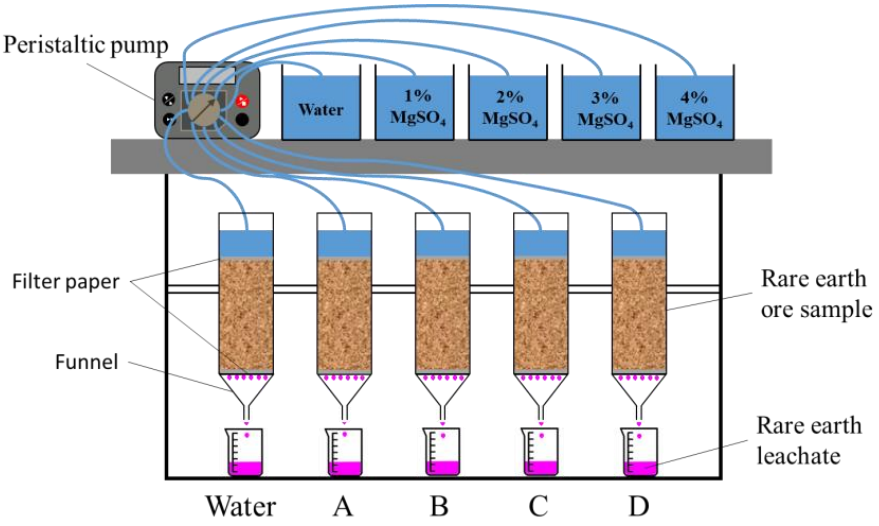

Figure 5. Expanded experiments of column leaching process.

The leaching efficiency of rare earth elements was calculated with the following formula:

$$\alpha = \frac{C \times V}{m \times \omega} \tag{22}$$

In this formula, α is the leaching efficiency of rare earth elements (%); C is the concentration of rare earth elements in the collected leach liquor (g/L); V is the volume of collected leach liquor (L); m is the mass (g) of the rare earth samples prior to ore leaching; ω is the grade (%) of rare earth samples prior to ore leaching.

3. Results and Discussion

3.1. Leaching Efficiency of Rare Earth Ions

In the pilot column leaching test, Figure 6 shows the concentration–time curve and leaching efficiency–time curve of rare earth ions in the leach liquor leached with different concentrations of $MgSO_4$. At the 300th minute, the leaching efficiencies of rare earth minerals with 1%, 2%, 3% and 4% concentration of magnesium sulfate are 84.16%, 94.65%, 97.24% and 97.98% respectively. It can be seen that when conducting leaching experiments with a 1% $MgSO_4$ solution, in order to achieve a leaching efficiency of over 90%, the leaching period was much longer compared to 2%, 3% and 4%. The total amount of leaching solution required during the leaching process also increased, which not only increased the difficulty and intensity of tasks such as precipitation and impurity removal but also increased the water circulation workload in the mining area to achieve a leaching efficiency of over 90% for ion-adsorbed REEs.

The experiments revealed that the peak concentration of rare earth ions in leach liquor increased with the rising $MgSO_4$ concentration. In other words, the rising concentration of $MgSO_4$ solution is conducive to the leaching of rare earth ions. In the column leaching test, Mg^{2+} in the leaching solution continuously reacted with rare earth cations. The growing concentration of $MgSO_4$ increased the Mg^{2+} contents in the leaching solution, which boosted the amount of RE^{3+} that reacts with the $MgSO_4$ solution, thus expanding the peak contents of rare earth ions in the leaching solution.

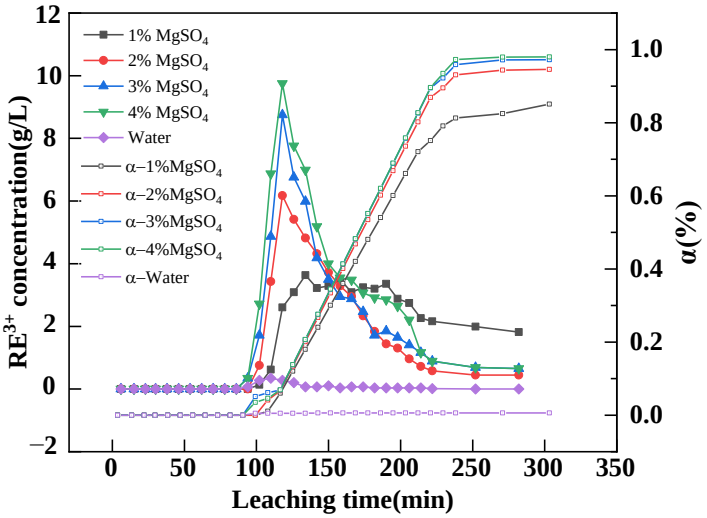

Figure 6. RE^{3+} concentration and leaching efficiency.

Leaching with $MgSO_4$ with a concentration of 4%, the peak concentration of rare earth ions in the leaching solution was obviously higher than that that obtained from leaching with $MgSO_4$ with a concentration of 3%. It shows that the overall ion exchange reaction rate of the column leaching test samples increased obviously with the rising concentration of the $MgSO_4$ solution.

In the pilot column leaching test, the variation of leached rare earth ion concentration with the passage of time is consistent with the results of previous research [40]. Thus, we can conclude that the column leaching test results are reliable.

3.2. Mass Transfer Analysis of Rare Earth Ions

Applying $MgSO_4$ solution with the concentrations of 1%, 2%, 3% and 4%, we performed the column leaching experiments. The testing results correspond, respectively, to the test groups of A, B, C and D. The penetration time is the first seepage time when there are no rare earth ions in the seepage liquid of the leaching solution. Table 6 shows the breakthrough time for each group. It can be seen that the concentration of the $MgSO_4$ solution clearly effected the permeability of the leaching solution. The lower the concentration of the $MgSO_4$ solution, the faster the leaching solution permeated in the ore body. Therefore, $MgSO_4$ solution with a low concentration has a shorter penetration time. For instance, the penetration time of test column D is 53.85% longer than that of column A.

Table 6. Penetration Time for Column Leaching.

Ore Pillar Number	Leaching Concentration/%	Time of First Seepage/h
A	1	39
B	2	41
C	3	57
D	4	61

As one of the major factors effecting the permeability of ore bodies, the dynamic viscosity of solution is inversely proportional to the infiltration flow [41]. Thus, the dynamic viscosity of its solution increases with the addition of $MgSO_4$ concentration. At a temperature of 25 °C, the traditional Ubbelohde viscosity method was applied to measure the density and dynamic viscosity of leaching solutions of different concentrations. Table 7 shows the results. Under a certain injection intensity, the infiltration flow of the $MgSO_4$ solution in ionic rare earth ore bodies is inversely proportional to the concentration of $MgSO_4$. The infiltration flow decreases with the rising $MgSO_4$ concentration. That said, the higher the concentration of the $MgSO_4$ solution, the greater the dynamic viscosity of

the solution and the slower the infiltration speed of the leaching solution in the rare earth ore bodies.

Table 7. Density and dynamic viscosity of $MgSO_4$ solutions with different mass concentrations.

Concentration of Leaching Solution	Density/(g/cm^3)	Dynamic Viscosity/(mPa.s)
1%	1.012	0.89538
2%	1.018	0.89609
3%	1.034	0.94731
4%	1.056	0.99908

In its essence, the mass transfer process of in situ leaching of ionic rare earth ore consists of the following steps: the seepage flow of the $MgSO_4$ solution inside the ore body; the entrance of rare earth ions into the leaching solution through exchange and diffusion; the rising concentration of rare earth ions in the leaching solution, which then seeps downward with the mother solution [42]. Theoretically, raising the concentration of the $MgSO_4$ solution increases the solution viscosity, which reduces the seepage velocity of leaching solution. Thus, it hinders the seepage flow of the leaching solution in the ore body. However, the dispersion of ions has the functions of seepage flow and molecular diffusion in the process of ionic rare earth leaching. With the expansion of the $MgSO_4$ solution's concentration, the distribution difference of $MgSO_4$ in the ore bodies also increases, thus raising the diffusion rate and intensity of Mg^{2+}. Accordingly, the rising diffusion speed of the leaching solution on the surface of soil particles accelerates the ion exchange reaction speed and shortens the leaching process. A question arises here, however. Does the rising concentration of $MgSO_4$ solution improve or slow down the mass transfer rate? This question needs to be further investigated.

A good indicator is the transfer time of the solute mass, which specifies the difference between the moment when REEs are initially measured and the instant when the liquid seeps out for the first time in the A, B, C and D test columns. The results are shown in Figure 7. The transfer time of solute mass is shortened when the concentration of $MgSO_4$ is increased. In comparison with that of column A, the first seepage time of column D increases by 56.41% due to its higher solution viscosity and slower seepage velocity (mechanical escape velocity). A rising concentration pressure difference of the $MgSO_4$ solution in the ore body raises the diffusion speed of molecules in the solution, which shortens the overall mass transfer time of column D in the ore body by 196.08%, in comparison with that of column A.

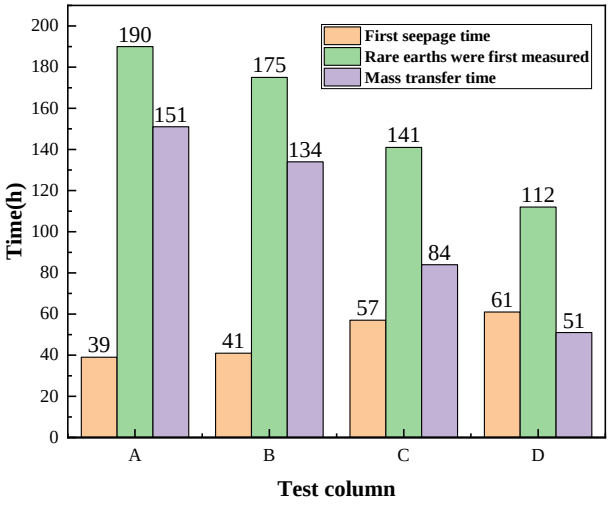

Figure 7. Mass transfer time for each test column.

It shows that the improvement effect generated by the rising leaching agent concentration is greater than the hindrance caused by dynamic viscosity. That is to say, the increasing mass transfer speed accelerates the leaching process.

3.3. Control Equation of Leaching Kinetics

In the ionic rare earth minerals, the impurities, such as Al^{3+}, Ca^{2+} and Fe^{2+}, are relatively low in their chemical activity. In the initial stage of leaching, the impurity ions take a precedence over rare earth ions in their chemical replacement with Mg^{2+} ions in the leaching solution. Therefore, they exert a certain adverse effect on the leaching effect of rare earths. As a result, the reducing leaching efficiency of rare earth and the rising consumption of leaching agents negatively influence the leaching process. During the in situ leaching of ionic rare earth, particularly its final phase, there exists a tailing phenomenon. Therefore, the leaching curve of rare earth ions has a long trailing stage in the late stage of leaching. In view of this, the experimental data for rare earth leaching efficiencies lower than 5% and higher than 85% are included in this research.

Upon analyzing the data with the dynamic equation of external diffusion control, we established the relationship between (α) and leaching time (t), as shown in Figure 8. Outside the control of external diffusion, the leaching efficiency of RE demonstrates no obvious linear relationship with leaching time when the concentration of $MgSO_4$ is 1%, with the value of the linear coefficient (R^2) being 0.976. When the concentration of $MgSO_4$ is 2%, 3% and 4%, there exists a linear relationship between rare earth leaching efficiency and leaching time. Under these circumstances, the values of the linear coefficient (R^2) are above 0.99. In other words, the external diffusion plays a dominant role in the leaching of rare earth when the concentration of $MgSO_4$ is 2% or higher. In the figure, the straight line α–t does not pass through the origin point. It can be accounted for by the following aspects: on the one hand, it takes time for $MgSO_4$ to seep between pores; on the other hand, the impurity ions, such as Al^{3+}, Ca^{2+} and Fe^{2+}, take precedence over rare earth ions in their reaction with $MgSO_4$. As a result, we observed the phenomenon of delayed ore extraction (the absence of rare earth ion leaching) in the early stage of leaching.

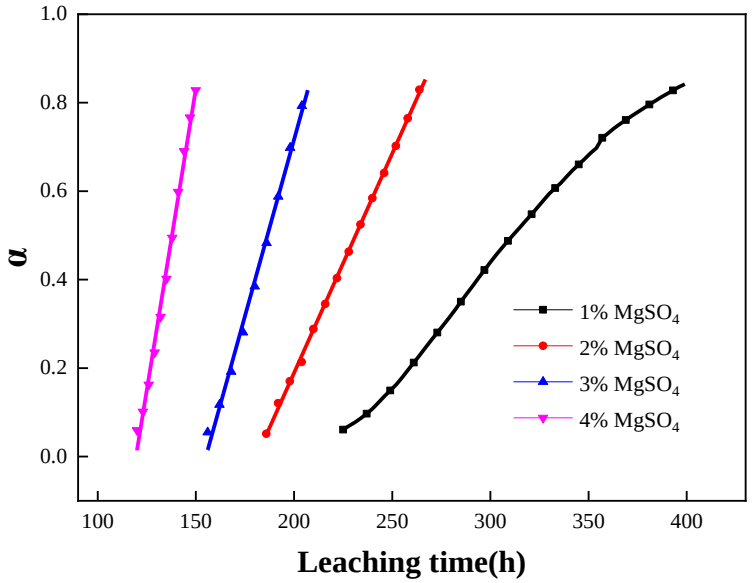

Figure 8. Fitting relationship between α and time t.

Upon analyzing the data with the dynamic equation of internal diffusion control, we established the relationship between $1 - \frac{2}{3}\alpha - (1-\alpha)^{\frac{2}{3}}$ and leaching time (t), as shown in Figure 9. In the whole leaching process, the curves are not completely linear. Therefore, the process is not regulated by internal diffusion.

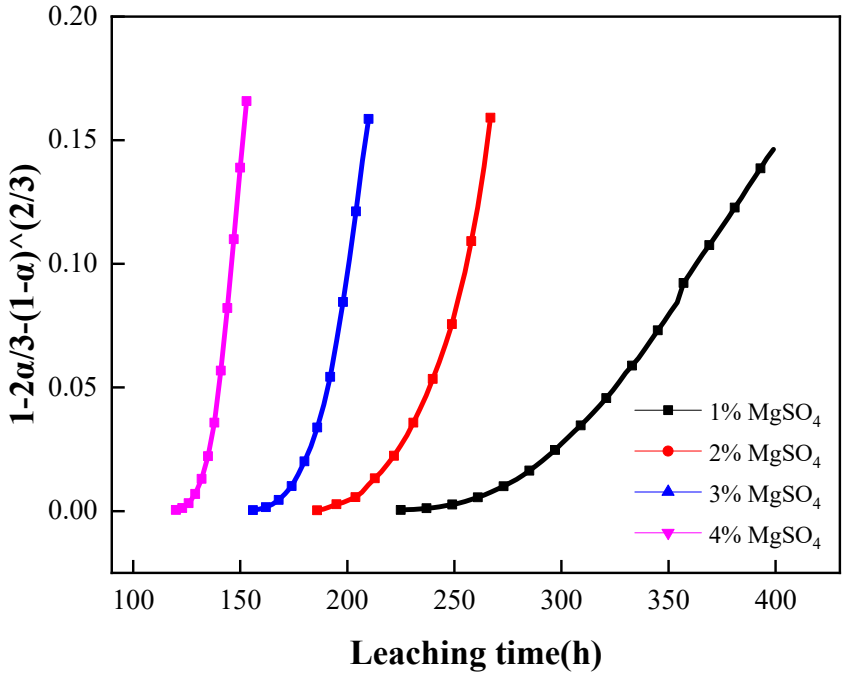

Figure 9. Fitting relationship between $1 - \frac{2}{3}\alpha - (1-\alpha)^{\frac{2}{3}}$ and time (t).

Upon processing the experimental data with the kinetic equation controlled by chemical reaction, we established the relationship between $1-(1-\alpha)^{\frac{1}{3}}$ and leaching time (t), as shown in Figure 10. The results of the four tests failed to reach a good linear relationship. Therefore, the kinetic processes leached with the four concentrations of $MgSO_4$ were not subject to the control of chemical reaction.

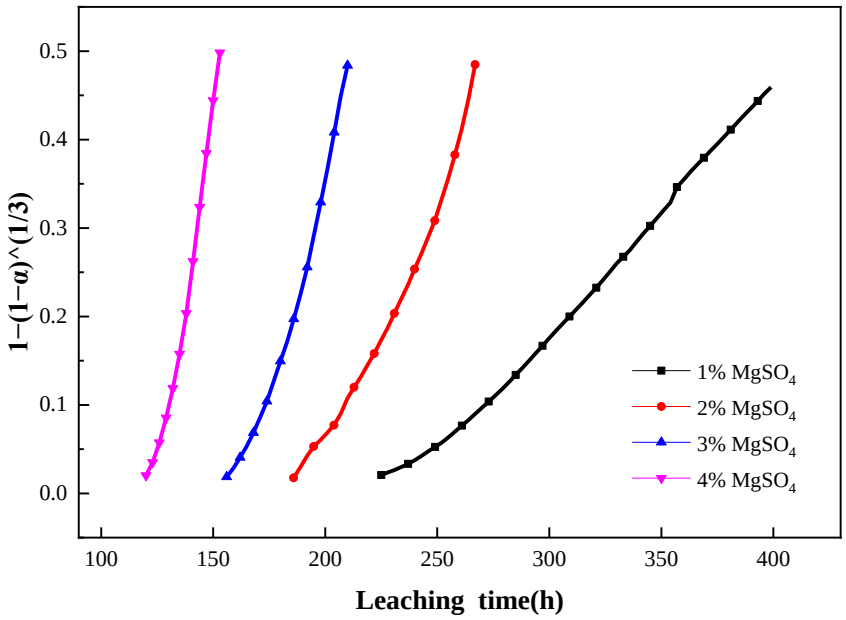

Figure 10. Fitting relationship between $1-(1-\alpha)^{\frac{1}{3}}$ and time (t).

In this leaching experiment with natural particle-sized RE particles, the changing concentrations of the $MgSO_4$ solution has a certain impact on the leaching kinetics control mode of rare earth. When $MgSO_4$ solution with a concentration of 1% is applied, the three processing methods of leaching data and leaching time are not linear. It can be defined as a complex mixed control mode. When $MgSO_4$ solutions with a concentration of 2%, 3% and

4% are employed for ore leaching, the leaching process is subject to external diffusion, with relatively low internal diffusion resistance.

As a multi-particle and mixed deposit with clay minerals as the major component, rare earth ore is characterized by small-sized particles. Due to the "dead-end pores" in the rare earth deposit structure, there are dominant areas and non-dominant areas in the ore body. The leaching solution in the non-dominant region lacks the capacity of completing the whole convection process [43]. The "liquid film" in the non-dominant area in the column leaching test is similar to the liquid film layer in the above-mentioned "shrinking core model". On the one hand, the effective thickness of the liquid film formed by the combination of multiple particles in the column leaching test is larger than that of the single particle size model. On the other hand, the long journey of Mg^{2+} diffusion from the leaching solution through the liquid film layer restricts the diffusion rate, which explains the reason why external diffusion becomes its main control process.

In the column leaching process, the increasing collection of rare earth ions to the lower part of the pore pillar lowers the exchange zone. First, the whole pillar reaches a saturation state until the completion of the mass transfer process of rare earth. After the pillar is saturated, the newly added leaching solution into the system maintains the concentration of Mg^{2+} in a constant state. Accordingly, the Mg^{2+} concentration in the exchange zone increases. Its concentration gradient is maintained at a high level, which further enhances the diffusion capacity of Mg^{2+} and accelerates its internal diffusion rate. The leaching of rare earth ions transforms from external diffusion control to mixed control when the internal diffusion rate of solute around the RE deposit particles is basically identical with the external diffusion rate.

Table 8 shows the control mode and kinetic control equation of natural particle-sized rare earth ions leached with different concentrations of $MgSO_4$.

Table 8. Leaching kinetics equation with different concentrations of $MgSO_4$.

$MgSO_4$ Concentration	Control Mode	Control Equation
1%	Hybrid control	$\frac{\mu\delta}{D_1}\alpha + \frac{3\mu r}{2D_2}\left[1 - \frac{2}{3}\alpha - (1-\alpha)^{\frac{2}{3}}\right] = \frac{3C_0M}{\rho r}$
2%	External diffusion control	$\alpha = kt$
3%	External diffusion control	$\alpha = kt$
4%	External diffusion control	$\alpha = kt$

4. Conclusions

By performing column leaching tests, we studied the kinetic process of leaching natural-sized rare earth particles with $MgSO_4$ on the basis of the "shrinking core model" theory. Upon analyzing the factors effecting the mass transfer process, the effects of various $MgSO_4$ concentrations on rare earth leaching kinetics were discussed. The suitable dynamic control mode of the leaching process with different concentrations of $MgSO_4$ provides a theoretical basis for the numerical simulation of leaching rare earth. We have obtained the following conclusions:

(1) In accordance with the results of ore pillar leaching experiments, the penetration time of RE leaching tests by using $MgSO_4$ with a concentration of 4% is 53.85% longer than that of 1%. The concentration of $MgSO_4$ is directly proportional to the dynamic viscosity and conversely proportional to the seepage velocity. Unfavorably to the saturation of the ore body, the application of high $MgSO_4$ concentration extends the leaching period. However, the rising concentration of $MgSO_4$ in the leaching system accelerates the diffusion speed of molecules in the solution, which is beneficial to the transport of solute. In comparison with the mass transfer time when $MgSO_4$ with a concentration of 1% is used as the leaching agent, the mass transfer time of $MgSO_4$ with a concentration of 4% is only 33.77%. The effect of increasing the leaching agent concentration on improving the mass transfer speed is larger than the hindrance caused by dynamic viscosity.

(2) When the concentration of $MgSO_4$ is 2% or higher, the rare earth leaching efficiencies in the ore pillar leaching tests reach above 90%, with the values of the leaching efficiencies being 94.65%, 97.24% and 97.98%, respectively, when the concentrations of $MgSO_4$ are 2%, 3% and 4%. Theoretically, an increase in $MgSO_4$ concentration within a certain range expands the Mg^{2+} concentration gradient difference per unit volume, which promotes the positive progress of the ion exchange reaction and improves the leaching efficiency of rare earths.

(3) When the concentrations of $MgSO_4$ are 3% and 4%, the rare earth leaching efficiencies show a slight difference, being 97.24% and 97.98%, respectively. The residual $MgSO_4$ amount in the wake of the leaching process shall be considered by determining an appropriate concentration of $MgSO_4$. As one of the important cost indicators of rare earth mining, it effects the relationship between leaching agent inputs and rare earth outputs.

(4) On the basis of the "shrinking core model" theory, the results of analyzing the leaching process of different concentrations of $MgSO_4$ show that when the $MgSO_4$ solution with a concentration of 1% is applied for RE deposit leaching, the leaching process can be described by a hybrid control kinetic equation. When the $MgSO_4$ solution with concentrations of 2%, 3% and 4% are used for ore leaching, their leaching processes can be described by the kinetic equation of external diffusion control.

Author Contributions: Conceptualization, M.H., D.W. and Y.R.; methodology, D.W.; software, W.N.; validation, M.H., W.X. and D.W.; formal analysis, M.H. and D.W.; investigation, W.X. and M.H.; resources, Y.R.; data curation, M.H.; writing—original draft preparation, M.H.; writing—review and editing, Y.R. and W.N.; visualization, M.H.; supervision, D.W.; project administration, Y.R.; funding acquisition, Y.R. All authors have read and agreed to the published version of the manuscript.

Funding: This research was funded by the National Natural Science Foundation of China, grant number 51964014.

Data Availability Statement: The data that support the findings of this study are available from the corresponding author upon reasonable request.

Conflicts of Interest: The authors declare no conflict of interest.

References

1. Yang, X.; Lin, A.; Li, X.; Wu, Y.; Zhou, W.; Chen, Z. China's ion-adsorption rare earth resources, mining consequences and preservation. *Environ. Dev.* **2013**, *8*, 131–136. [CrossRef]
2. Wang, C.; Wang, L.; Li, L. A leaching experiment on different grades of ion-adsorbed rare earth deposits $(NH_4)_2SO_4/MgSO_4$. *Rare Earthv.* **2018**, *39*, 67–74. [CrossRef]
3. Mory, T.; Gong, A.; Wang, Y.; Qiu, L.; Bai, Y.; Zhao, W.; Liu, Y.; Chen, Y.; Liu, Y.; Wu, H.; et al. Research progress of rare earth separation methods and technologies. *J. Rare Earths* **2023**, *41*, 182–189. [CrossRef]
4. Laís, N.V.; Ana, P.S.S.; Daniel, L.G.; Wendy, J.S.R.; Tatiana, D.S. Fluorescent lamps: A review on environmental concerns and current recycling perspectives highlighting Hg and rare earth elements. *J. Environ. Chem. Eng.* **2022**, *10*, 108915. [CrossRef]
5. Wang, D.; Rao, Y.; Han, M.; Shi, L.; Liu, L.; Zhang, M. Warning Model of the Ionic Rare Earth Mine Slope Based on Creep Deformation Time Series. *Geofluids* **2021**, *11*, 2236476. [CrossRef]
6. Chi, R.; Liu, X. Prospect and Development of Weathered Crust Elution-Deposited Rare Earth Ore. *J. China Rare Earth* **2019**, *37*, 129–140.
7. Luo, X.; Weng, C.; Xu, J.; Ma, P.; Tang, X.; Chi, R. Research Progress on and Development Trend of Exploitation Technique of Ion-absorbed Type Rare Earth Ore. *Met. Mine* **2014**, *6*, 83–90.
8. Wu, Z.; Chen, Y.; Wang, Y.; Xu, Y.; Lin, Z.; Liang, X.; Cheng, H. Review of rare earth element (REE) adsorption on and desorption from clay minerals: Application to formation and mining of ion-adsorption REE deposits. *Ore Geol. Rev.* **2023**, *157*, 105446. [CrossRef]
9. Guo, Z.; Zhao, K.; Jin, J. Reviews on Environmental Assessment and Pollution Prevention of Ion Adsorption Type Rare Earth Ores. *Rare Earth* **2019**, *40*, 115–126. [CrossRef]
10. Yang, X.; Xi, G.; Yao, N.; Zhou, M.; Gao, X.; Chen, M.; Wang, X.; Pan, Z.; Wang, Z. Spatiotemporal distribution of residual ammonium in a rare-earth mine after in-situ leaching: A modeling study with scarce data. *J. Hydrol.* **2022**, *615*, 128669. [CrossRef]
11. Zhang, Q.; Ren, F.; Li, F.; Chen, G.; Yang, G.; Wang, J.; Du, K.; Liu, S.; Li, Z. Ammonia nitrogen sources and pollution along soil profiles in an in-situ leaching rare earth ore. *Environ. Pollut.* **2020**, *267*, 115449. [CrossRef] [PubMed]

12. Zhang, J.; Hu, F.; Liu, Z. Study on the Migration of Ammonium Nitrogen in the Soil of the Ionic Type Rare Earth Ore Area. *Rare Earth* **2018**, *39*, 108–116. [CrossRef]
13. Yang, L.; Li, C.; Wang, D.; Li, F.; Liu, Y.; Zhou, X.; Liu, M.; Wang, X.; Li, Y. Leaching ion adsorption rare earth by aluminum sulfate for increasing efficiency and lowering the environmental impact. *J. Rare Earths* **2019**, *37*, 429–436. [CrossRef]
14. Luo, X.; Yuan, X.; He, K.; Zhang, Y.; Luo, C.; Liu, Z.; Zhou, H. Precipitation process for combined impurity removal from a magnesium sulphate-based leachate of ionic rare earth ore. *Miner. Eng.* **2022**, *189*, 107911. [CrossRef]
15. Yin, S.; Pei, J.; Jiang, F.; Li, S.; Peng, J.; Zhang, L.; Ju, S.; Srinivasakannan, C. Ultrasound-assisted leaching of rare earths from the weathered crust elution-deposited ore using magnesium sulfate without ammonia-nitrogen pollution. *Ultrason. Sonochemistry* **2018**, *41*, 156–162. [CrossRef] [PubMed]
16. Wang, R.; Xie, B.; Pan, Y. Selection of Leaching Agent and Optimization of Column Leaching Process of Ion-Absorbed Rare Earth Deposits. *Rare Met.* **2015**, *39*, 5. [CrossRef]
17. Huang, X.; Yu, Y.; Feng, Z.; Zhao, N. A Method of Recovering Rare Earth from Ion-Adsorbed Rare Earth Deposits. China Patent CN 201010128302.9, 21 September 2011.
18. Xiao, Y.; Feng, Z.; Huang, X.; Huang, L.; Chen, Y.; Liu, X.; Wang, L.; Long, Z. Recovery of rare earth from the ion-adsorption type rare earths ore: II. Compound leaching. *Hydrometallurgy* **2016**, *163*, 83.
19. Yi, Q.; Zhang, Y.; Zhao, Q.; Zhang, X. A Method of Extracting Rare Earth Oxides from Rare Earth Minerals. China Patent CN 202110883699.0, 3 December 2021.
20. Chen, K.; Pei, J.; Yin, S.; Li, S.; Peng, J.; Zhang, L. Leaching behaviour of rare earth elements from low-grade weathered crust elution-deposited rare earth ore using magnesium sulfate. *Clay Miner.* **2018**, *53*, 505–514. [CrossRef]
21. Chen, X.; He, Q.; Chen, J.; Huang, L.; Tan, C.; Yin, Y.; Jiao, Y.; Xiao, Y. Development of Leaching Technology and Theory of Ion-Adsorption Type Rare Earth Ore. *J. China Rare Earth* **2022**, *40*, 936–947.
22. Bo, F.; Zhao, L.; Feng, Z.; Liu, D.; Yin, W.; Long, Z.; Huang, X. Leaching behaviors of calcium and magnesium in ion-adsorption rare earth tailings with magnesium sulfate. *Trans. Nonferrous Met. Soc. China* **2021**, *31*, 288–296. [CrossRef]
23. Huang, J.; Yang, Y.; Deng, Y.; Wang, L.; Wang, H.; Huang, Z. Leaching Kinetics of Ionic Rare Earth Ore with Magnesium Sulfate. *Rare Met.* **2022**, *46*, 265–272. [CrossRef]
24. Xu, Q.; Sun, Y.; Yang, L.; Li, C.; Zhou, X.; Chen, W.; Li, Y. Leaching mechanism of ion-adsorption rare earth by mono valence cation electrolytes and the corresponding environmental impact. *J. Clean. Prod.* **2019**, *211*, 566–573. [CrossRef]
25. Meng, X.; Zhao, H.; Zhang, Y.; Shen, L.; Gu, G.; Qiu, G.; Zhang, X.; Yu, H.; He, X.; Liu, C. Simulated bioleaching of ion-adsorption rare earth ore using metabolites of biosynthetic citrate: An alternative to cation exchange leaching. *Miner. Eng.* **2022**, *189*, 107900. [CrossRef]
26. Long, P.; Wang, G.; Zhang, C.; Huang, Y.; Luo, S. A two-parameter model for ion exchange process of ion-adsorption type rare earth ores. *J. Rare Earths* **2020**, *38*, 1251–1256. [CrossRef]
27. Long, P.; Wang, G.; Zhang, C.; Yang, Y.; Cao, X.; Shi, Z. Kinetics model for leaching of ion-adsorption type rare earth ores. *J. Rare Earths* **2020**, *38*, 1354–1360. [CrossRef]
28. Ghosh, A.; Ray, H.S. *Principles of Extractive Metallurgy*, 2nd ed.; Wiley Eastern Ltd.: New Delhi, India, 1991.
29. Zhou, F.; Liu, Q.; Feng, J.; Su, J.; Liu, X.; Chi, R. Role of initial moisture content on the leaching process of weathered crust elution-deposited rare earth ores. *Sep. Purif. Technol.* **2019**, *217*, 24–30. [CrossRef]
30. Feng, J.; Zhou, F.; Chi, R.; Liu, X.; Xu, Y.; Liu, Q. Effect of a novel compound on leaching process of weathered crust elution-deposited rare earth ore. *Miner. Eng.* **2018**, *129*, 63–70. [CrossRef]
31. Xiao, Y.; Feng, Z.; Hu, G. Leaching and mass transfer characteristics of elements from ion-adsorption type rare earth ore. *Rare Met.* **2015**, *34*, 357–365. [CrossRef]
32. Su, X.; Wang, Y.; Su, J.; Lai, W.; Gao, Y.; Sun, X. Enrichment of rare earths in magnesium sulfate leach solutions of ion-absorbed ores by extraction-precipitation. *Hydrometallurgy* **2019**, *189*, 105119. [CrossRef]
33. Jamal, A.B.; Sara, A.H.; Brahim, A.; Rachid, B.; Redouane, B.; Rachid, B. Kinetics and mechanisms of leaching of rare earth elements from secondary resources. *Miner. Eng.* **2022**, *177*, 107351. [CrossRef]
34. Souza, A.D.; Pina, P.S.; Lima, E.V.O.; Silva, C.A.D.; Leão, V.A. Kinetics of sulphuric acid leaching of a zinc silicate calcine. *Hydrometallurgy* **2007**, *89*, 337–345. [CrossRef]
35. Havlík, T. Kinetics of Heterogeneous Reactions of Leaching Processes. In *Hydrometallurgy*; Woodhead Publishing: Cambridge, UK, 2008; pp. 184–241. [CrossRef]
36. Wang, X.; Zhuo, Y.; Deng, S.; Li, Y.; Zhong, W.; Zhao, K. Experimental Research on the Impact of Ion Exchange and Infiltration on the Microstructure of Rare Earth Orebody. *Adv. Mater. Sci. Eng.* **2017**, *2017*, 4762858. [CrossRef]
37. Yin, S.; Chen, X.; Yan, R.; Wang, L. Pore Structure Characterization of Undisturbed Weathered Crust Elution-Deposited Rare Earth Ore Based on X-ray Micro-CT Scanning. *Minerals* **2021**, *11*, 236. [CrossRef]
38. *GB/T 14635-2008*; General Administration of Quality Supervision, Inspection and Quarantine of the People's Republic of China, Standardization Administration of China. Rare Earth Metals and Their Compounds. Determination of Total Rare Earth Contents. China Standards Press: Beijing, China, 2008.
39. *GB/T 50123–2019*; Ministry of Housing and Urban-Rural Development, People's Republic of China, China's State Administration for Market Regulation. Standards for Geotechnical Test Methods. China Planning Press: Beijing, China, 2019.

40. Zhou, L.; Wang, X.; Huang, C.; Wang, H.; Ye, H.; Hu, K.; Zhong, W. Development of pore structure characteristics of a weathered crust elution-deposited rare earth ore during leaching with different valence cations. *Hydrometallurgy* **2021**, *201*, 105579. [CrossRef]
41. Zeng, S.; Song, J.; Sun, B.; Wang, F.; Ye, W.; Shen, Y.; Li, H. Seepage characteristics of the leaching solution during in situ leaching of uranium. *Nuclear Eng. Technol.* **2023**, *55*, 566–574. [CrossRef]
42. Liu, C.; Zhou, F.; Wu, X.; Feng, J.; Chi, R. Development and Prospect in Seepage and Mass Transfer Process of Weathered Crust Elution-Deposited Rare Earth Ore. *Rare Earth* **2021**, *42*, 111–121.
43. Yuan, Q. Fluid retention on miscible viscous fingering of finite slices in porous media with dead-end pores. *Chem. Eng. Sci.* **2022**, *263*, 118060. [CrossRef]